

Supporting Information

Spontaneous resolution of 3D chiral polyoxometalate-based polythreaded framework consisting of achiral ligand

Ya-Qian Lan, Shun-Li Li, Zhong-Min Su,* Kui-Zhan Shao, Jian-Fang Ma,*
Xin-Long Wang and En-Bo Wang*

Institute of Functional Material Chemistry; Key Lab of Polyoxometalate Science of Ministry of Education, Faculty of Chemistry, Northeast Normal University, Changchun, 130024, China.

E-mail: zmsu@nenu.edu.cn; jianfangma@yahoo.com.cn; wangenbo@public.cc.jl.cn;
Tel: +86 431 85099108

The bond valence sum calculations for L-1 and D-1:

The bond valence sums (BVS)^[1] are 4.415, 5.152, 5.135, 5.167, 5.256, 5.020, 5.090, 4.370, 5.138 and 5.100 for ten independent vanadium atoms (V1-V10), respectively, in L-1. While the corresponding values are 4.400, 5.161, 5.142, 5.156, 5.294, 5.129, 5.084, 4.396, 5.188 and 5.149 for ten independent vanadium atoms (V1-V10), respectively, in D-1. The calculated results reveal that, in the structure of the polyanion of L-1, two (V1 and V8) out of the ten vanadium centers are in the +4 oxidation state, and other vanadium centers (V2, V3, V4, V5, V6, V7, V9 and V10) are +5 oxidation state. This result is similar to that in the reported complexes.^[2-4] The values of BVS for Cu1, Cu2 and Cu3 centers are 1.557, 0.873 and 0.896 in L-1 and 1.579, 0.893 and 0.922 in D-1, respectively, suggesting that the Cu1 atom in L-1 exhibits an oxidation state of +2, and Cu2 and Cu3 atoms have an oxidation state of +1.

[1] The valence sum calculations are performed on a program of bond valence calculator, version 2.00 February 1993, written by C. Hormillosa with assistance from

S. Healy, distributed by I. D. Brown.

- [2] A. Bino, S. Cohen and C. Heitner-Wirguin, *Inorg. Chem.*, 1982, **21**, 429.
- [3] Y. Hayashi, N. Miyakoshi, T. Shinguchi and A. Uehara, *Chem. Lett.*, 2001, 170.
- [4] Y. G. Li, Y. Lu, G. Y. Luan, E. B. Wang, Y. B. Duan, C. W. Hu, Ni. H. Hu and H. Q. Jia, *Polyhedron*, 2002, **21**, 2601.

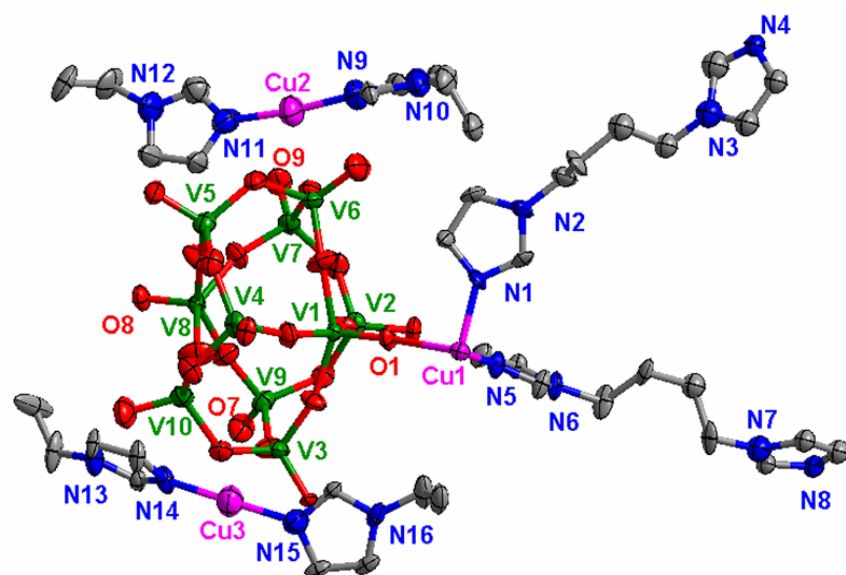


Figure S1. ORTEP diagram of the asymmetric unit of D-1 with thermal ellipsoids at the 30% probability displacement, the hydrogen atoms and water molecules are omitted for clarity.

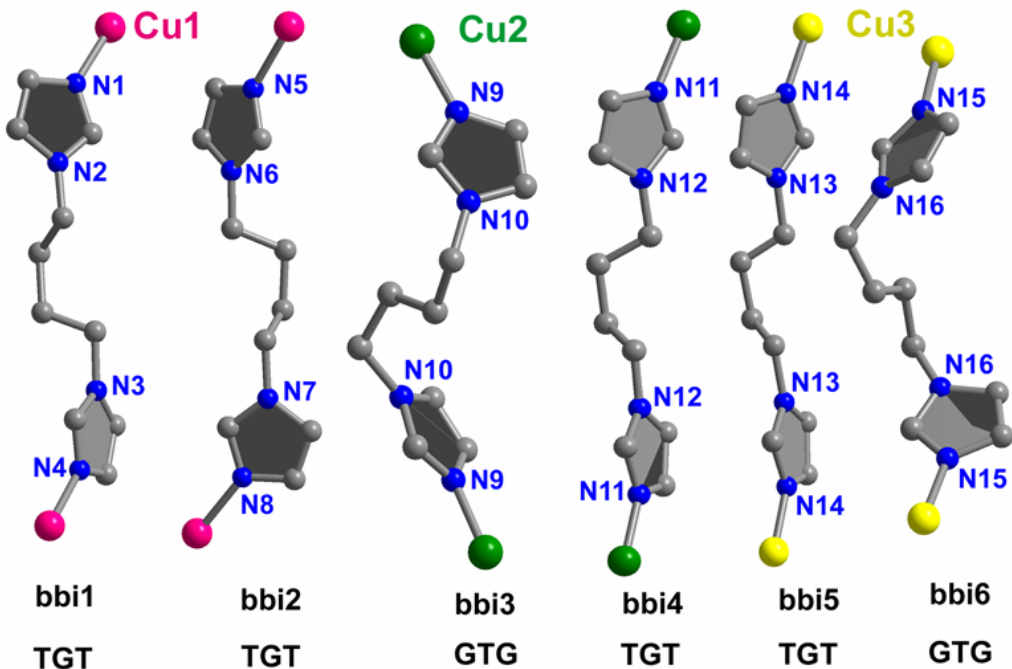


Figure S2. Ball-stick representation of the different conformations of six bbi ligands.

In compounds L-1 and D-1, there are six kinds of bbi ligands. They all adopt a bis-monodentate coordination mode to bridge two metal centers. The bbi1 and bbi2 coordinate to Cu1 cations and adopt TGT (T = trans, G = gauche) conformations with the dihedral angles between two imidazol rings of 33.4° and 33.0° , respectively. While the bbi3 and bbi4 coordinate to Cu2 ions with GTG and TGT conformations with the corresponding dihedral angles of 38.5° and 24.7° , respectively. And the bbi5 and bbi6 coordinate to Cu3 ions with the different TGT and GTG conformations with the corresponding dihedral angles of 26.5° and 37.2° , respectively.

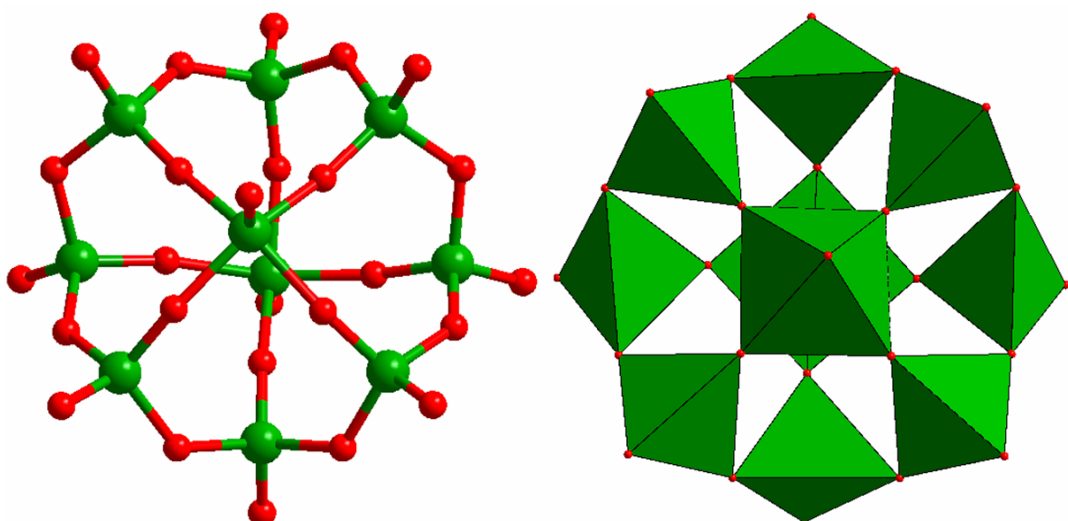


Figure S3. Ball-stick (a) and polyhedral (b) representations of $[V_{10}O_{26}]^{4-}$ polyoxoanion.

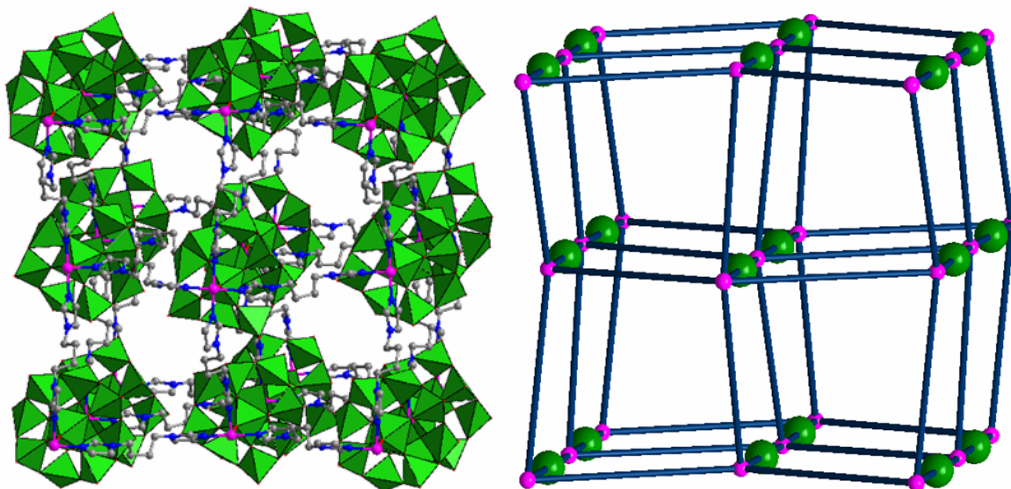


Figure S4. Schematic view of the twisted α -Po topology formed by Cu1, bbi1, bbi2 and $[V_{10}O_{26}]^{4-}$ polyoxoanion.

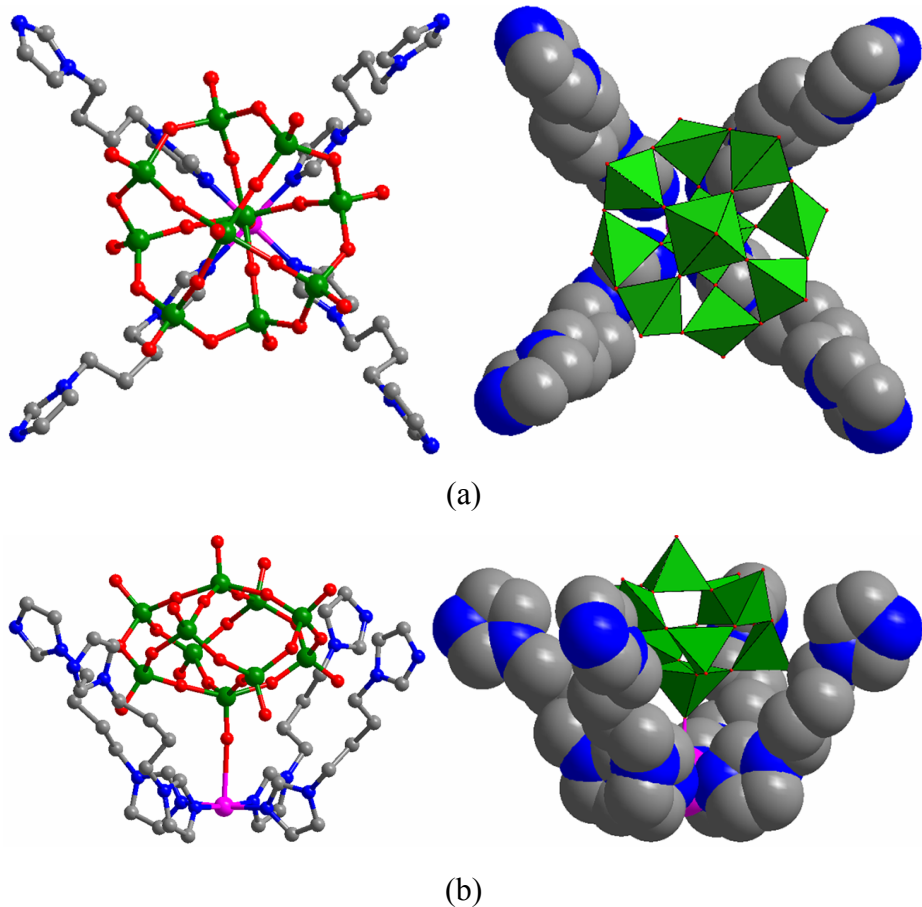


Figure S5. Ball-stick (left), and polyhedral and space-filling (right) representations of

a floriated subunit in which two bbi1 and two bbi2 ligands act as petal and $[V_{10}O_{26}]^{4-}$ polyoxoanion acts as stamen along the different directions in (a) and (b).

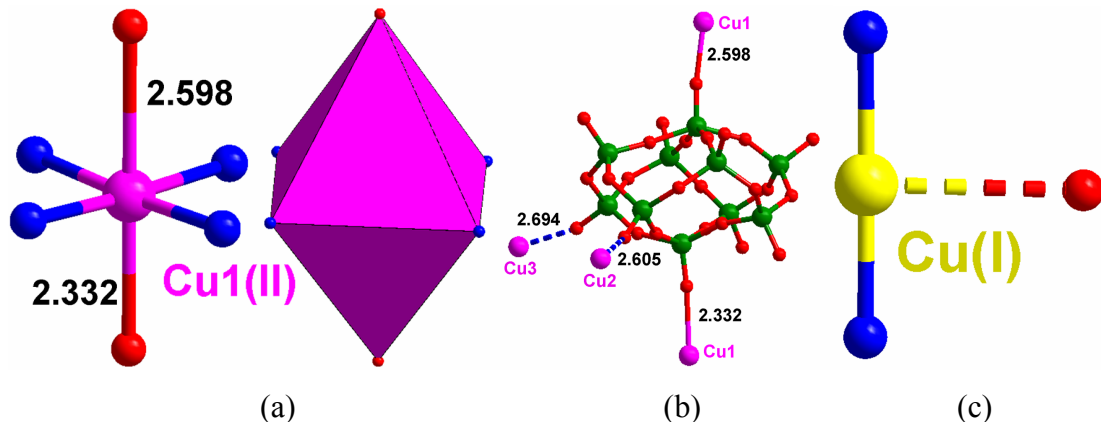


Figure S6. (a) Ball-stick and polyhedral representations of a 6-connected node $[Cu(II)]$. (b) Ball-stick representation of a $[V_{10}O_{26}]^{4-}$ polyoxoanion as a 4-connected node coordinating to two Cu1 cations with covalent bonds and Cu2 and Cu3 cations with Cu-O interactions. (c) View of a Cu(I) cation as a 3-connected node.

The Cu-O distances are slightly different in L-1 and D-1. (Cu1-O1 2.596 Å, Cu1-O8 2.331 Å, Cu2-O9 2.605 Å and Cu3-O7 2.694 Å in L-1, Cu1-O1 2.598 Å, Cu1-O8 2.332 Å, Cu2-O9 2.61 Å and Cu3-O7 2.697 Å in D-1.)

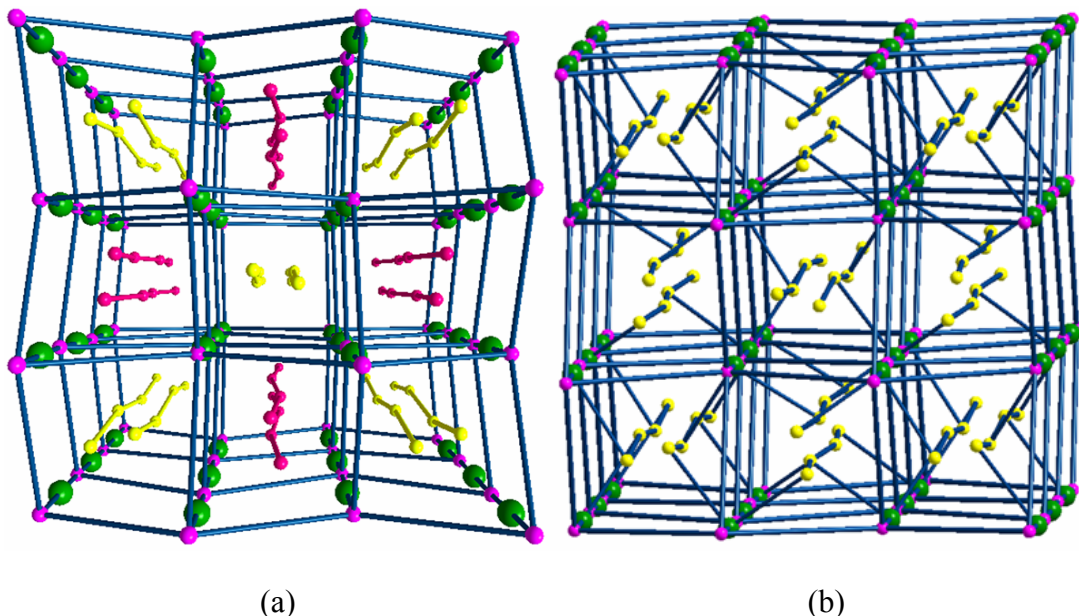


Figure S7. (a) Schematic representation of a polythreaded framework in compound 1. (b) Schematic representation of the (3,4,6)-connected framework with nodes and edges.

$(6.8^2)_2(6^5.8)(4^4.6^8.8^3)$ topology. (yellow, pink and green balls represent 3-, 4- and 6-connected nodes, respectively)

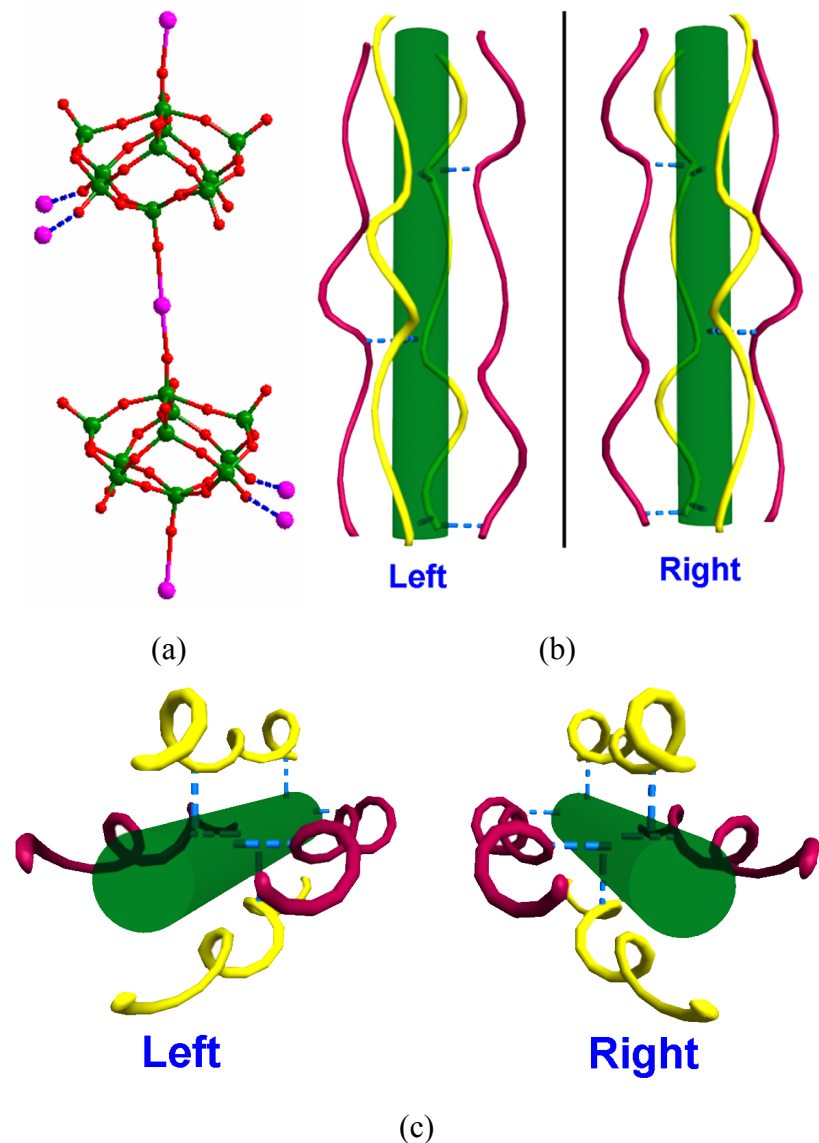


Figure S8. (a) Ball-stick representation of a $[\text{Cu}^{\text{II}}\text{Cu}^{\text{I}}_2\text{V}_{10}\text{O}_{26}]_{\infty}$ chain with a 2-fold screw axis. (b) and (c) Schematic view of the chiral subunit $[\text{Cu}^{\text{II}}\text{Cu}^{\text{I}}_2(\text{bbi})_2\text{V}_{10}\text{O}_{26}]_{\infty}$ along the different directions (left in L-1, right in D-1 and dashed lines represent Cu(I)-O interaction).

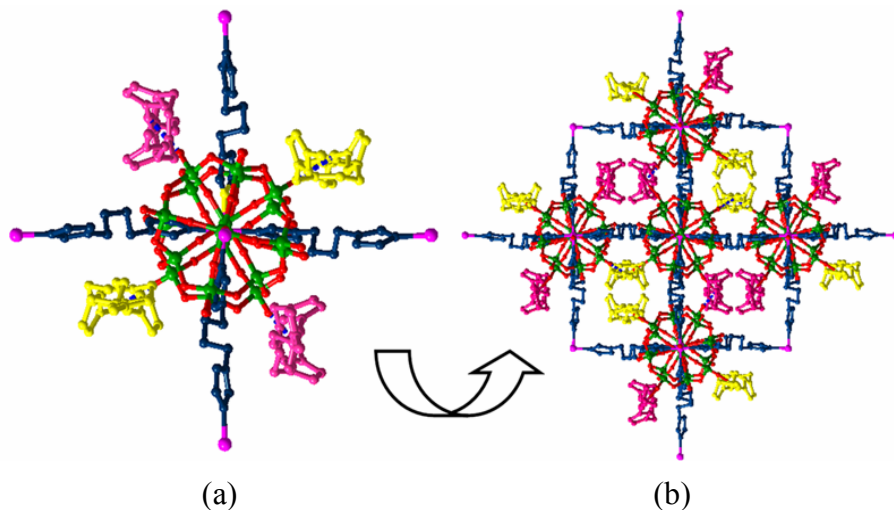


Figure S9. (a) Ball-stick representation of a chiral subunit $[\text{Cu}^{\text{II}}\text{Cu}^{\text{I}}_2(\text{bbi})_2\text{V}_{10}\text{O}_{26}]_{\infty}$ coordinating to four bbi ligands (two bbi1 and two bbi2) with similar conformations. (b) View of the whole 3D structure of D-1.

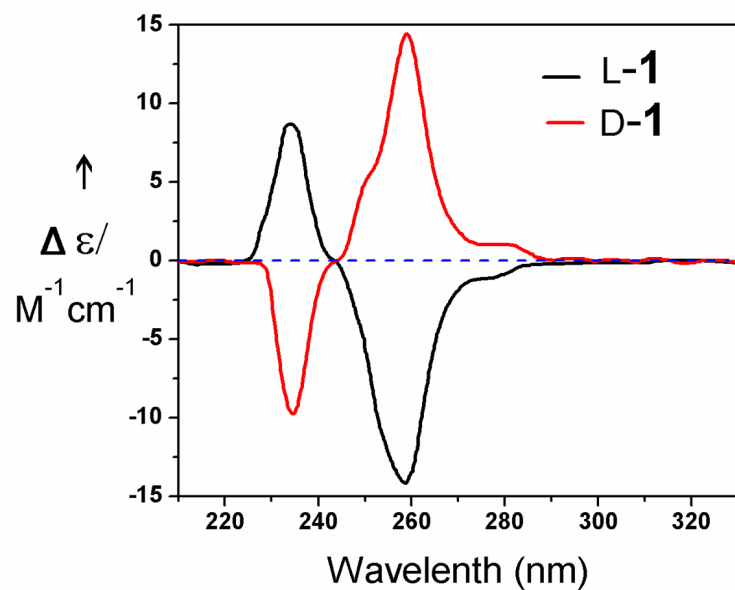


Figure S10. CD spectra of L-1 and D-1 in DMSO solution ($L-1 c = 8.0 \times 10^{-4} \text{ M}$, $D-1 c = 8.1 \times 10^{-4} \text{ M}$).

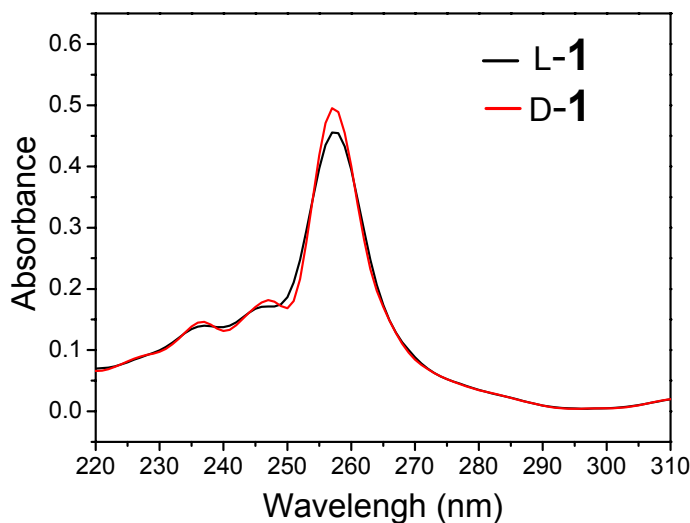


Figure S11. UV-Vis spectra of L-1 and D-1 in DMSO solution ($L-1 c = 1.45 \times 10^{-5}$ M, $D-1 c = 1.50 \times 10^{-5}$ M).

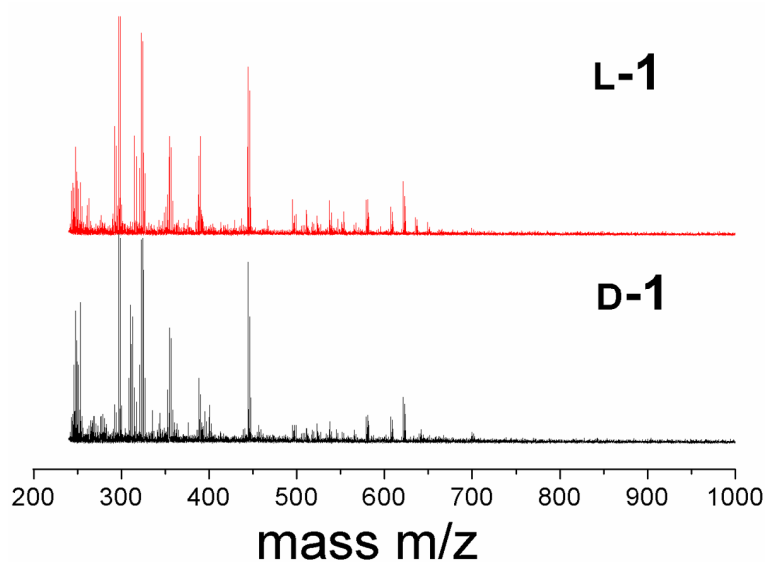


Figure S12. Electrospray ionization mass spectra of L-1 and D-1 in DMSO solution.

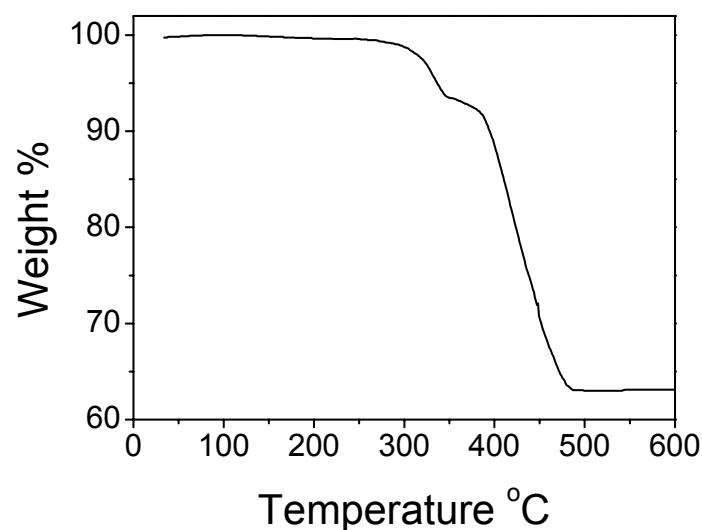


Figure S13. The TG curve of the mixture of L-1 and D-1. The compound 1 was stable up to 253°C.